Anti-erosion performance of asphalt pavement with a sub-base of cement-treated mixtures

Rui Guo [a,*], Tengfei Nian [b], Ping Li [b], Jiangtao Fu [a], Hong Guo [a]

[a] School of Civil Engineering and Architecture, Shaanxi University of Technology, Hanzhong 723000, China
[b] School of Civil Engineering, Lanzhou University of Technology, Lanzhou 730050, China

HIGHLIGHTS

- The relationship between anti-erosion performance of cement-treated mixtures and cement dosage, strength grade, and curing age has been further analyzed based on model experiment.
- The primary-secondary relationship of the main influencing factors on the scour resistance of cement-treated mixtures' scour resistance has been proved.
- A prediction model of cement-treated mixtures' scouring mass was established with the parameters of aggregate fractal dimension, cement dosage, water content, 28d cement mortar strength, and compaction, based on grey system theory.
- It gives suggestions on the best skeleton type of cement-treated mixtures for similar projects.

ARTICLE INFO

ABSTRACT

In this paper, the factors that affect the anti-erosion performance of three grades of cement-treated mixtures and their degree of association were studied using the Baohan highway in the Qinba mountain area, China as an engineering example. Firstly, the principal factors that affected changes in the anti-erosion performance of cement-treated mixtures and its law were analyzed with self-development model testing, which is considering changes in the aggregate's fractal dimension, compaction, cement dosage, curing age, water content, and cement strength grade in the mixtures. Secondly, the correlation coefficient between the influencing factors, scouring mass, and the predicted model for the cement-treated mixtures' scouring mass were developed according to the Grey Theory. The results showed that the mixtures' anti-erosion performance increased as cement content, strength, and curing age increased. Further, their anti-erosion performance increased firstly and then weakened with increased water content and compaction. In comparing cement-treated mixtures with suspended dense and skeleton voids, the former's scouring resistance was better. Among all these factors, the mixtures' structural type affected its erosion resistance greatly, while the cement strength grade had little effect. The cement-treated mixtures' scouring mass prediction model was established by combining material properties and external environmental factors, which can provide a reference for the design and construction of highways' base and subgrade in similar areas.

© 2019 Elsevier Ltd. All rights reserved.

1. Introduction

The increase in heavy traffic and the evolution of road transportation require road pavements with high structural performance [1]. Highway pavement is a multi-layered structure composed of a concrete or asphalt slab resting on a foundation system constituted of various layers, including the base, sub-base, and sub-grade [2].

The road base/sub-base is an important part of asphalt pavement structure, and its bearing capacity can be improved by replacing untreated granular layers with treated layers [3]. Many kinds of agents are used to stabilize road materials in applied engineering, including cement, lime, granulated blast furnace slag, bitumen, pozzolanas, and chemical stabilizers. Cement is recommended specifically because it increases aggregate graded mixtures' strength, cohesion, and durability effectively [4,5]. Cement-treated materials range from coarse-grained and recycled aggregates to very fine-grained soils [6].

---

* Corresponding author.
   E-mail addresses: grlch2356@163.com (R. Guo), hguo@sunt.edu.cn (H. Guo).

Cement-treated aggregate materials, which are compacted mixtures in which a relatively low dosage of cement is used to bind coarse aggregate, require a defined percentage of water content for both compaction and cement hydration. This technique was developed first in 1915, when a pavement in Sarasota, Florida, was constructed and compacted using a mixture of shells, sand, and Portland cement. Since then, cement-treated mixtures have been applied widely as road base/sub-base pavements in many countries [7,8]. Cement-treated materials' production can be divided into in-plant cement treatment and in situ cement stabilization. In-plant cement-treated materials are produced using natural or crushed aggregates, cement, and a defined percentage of water, and are used primarily in base courses. In situ cement stabilization is produced with a recycling train to spread the cement, a recycler to add water, a vibrating drum roller, and a grader for shaping and leveling, and is applied to deep layers (sub grade or sub-base courses) [1,9,10].

Generally, cement-treated aggregate materials used as road base material are designed as a heavy traffic base or a heavy traffic wearing course [11]. In applied engineering, the material treated as a base layer is applied widely in road engineering, largely to achieve the following goals [12]: ① improve road materials' workability; ② increase the mixture's strength; ③ enhance the pavement's durability; ④ increase the load spreading capacity; ⑤ good plate-forming properties, and ⑥ take full advantage of local materials. Because of these advantages, cement-treated mixtures demonstrate good properties and a longer service life compared to unbound aggregate and flexible base layers. Accordingly, they have been used commonly as the sub-base in highway asphalt pavement in China since the 1980s [13], and continue to be developed and improved.

Cement-treated mixtures are fine sub-base materials with quite different properties and service life compared to unbound aggregate or flexible base layers. However, when their sub-base is formed, its internal structure has some cracks and micro-pores, and these micro-defects may evolve slowly into macro-cracks traffic loads and other environmental factors cause [14]. This slow degradation process [15] causes some inherent problems, such as deformation cracking and low erosion resistance that affect the stability and durability of the pavement above it and the emergence of cracks causes the pavement to lose continuity and provides ways for water to penetrate the surface [16].

It is acknowledged that the compressive strength is an important indicator of a sub-base of cement-treated mixtures' quality. A number of primary variables influences cement-treated mixtures' compressive strength, including the aggregate's gradation type, degree of compaction, cement and water content, and curing time [5]. The relations among them are described as follows: the relation between their compressive strength and the cement content is linear [17], and is determined by the aggregate type and the fines content. It has been found that as the degree of compaction increases, cement-treated mixtures' compressive strength increases [18]. The compressive strength continues to increase with the increase in water content up to a certain point, after which the compressive strength decreases [5]. Curing time is another important factor that affects these mixtures' compressive strength [12].

The water in cement-treated materials plays a significant role in cement hydration [19]. Cement-treated materials' compressive strength is attributed largely to cement hydrates' strength and the adhesive force between hydrated cement paste and aggregate and other materials. The ingress of water into the cement paste generates disjointing pressure [20] and reduces its strength. Water pressure is exerted under the action of high speed vehicles [21], and as a result, cement-treated mixtures deteriorate under the joint action of water and traffic, as a pressure gradient forms in the depth direction and pumps out the fine aggregate, weakening the base and sub-grade thereby.

Water damage is one of cement-treated mixtures bases' most common modes of failure. The scouring process in a cement-treated mixtures base can be divided into soaking and softening by free water, dissolution under hydrostatic pressure, and scouring under hydrodynamic pressure [22]. Most of the water collected on the pavement is discharged through the pavement drainage facilities, but when there is excessive water, or the surface drainage is hindered so that a small amount of water can infiltrate into the pavement structure along the cracks and accumulate at the bottom of the pavement base, it softens the surface material and reduces the bonding force between the material particles in the cement-treated mixtures sub-base [23]. When the cracks in the base are unconnected, pore-water pressure with the base material forms by the action of free water under traffic load, which accelerates the base materials' erosion, and results in shedding coarse aggregate on the top surface of the base. After the cracks penetrate throughout, the pulsating flow washes away the loose particles on the base surface easily, which is the reason that, under the action of vehicle load, the water in the crevices produces "pump suction", which has a scouring effect on the fine aggregate of the cement-treated materials base. The amount of fine aggregate increases gradually with scouring time, which reduces the binding power between the courses, decreases the base's structural capacity, and shortens the pavement's service life. In this process, the resistance decreases as the erosion damage accumulates, and eventually, the cement-treated base is damaged when the degree of erosion reaches a critical value. Thus, if the base's health status can be predicted and evaluated accurately, it can provide guidance for pavement design and maintenance [24].

Among the recent related studies on sub-grade water damage, only a small number has been devoted to evaluating cement-treated mixtures sub-bases' anti-erosion performance. Alexandria discussed the anti-brushing performance of different style cement-treated mixtures base courses in the laboratory and suggested that different gradation types influence their anti-erosion performance [25]. It has been demonstrated that fine aggregate's scouring mass in the cement-treated base composites increases linearly, while that of coarse aggregate increases rapidly in the early stage and slowly later [26]. Majarrez et al. (2014) suggested that the base needs to be protected by a specific thickness of bituminous layers to provide protection against water [27]. Further, Guo et al. (2018) analyzed cement-treated mixtures and lime-fly ash bases' anti-erosion performance and showed that with an increase in erosion time, the base's residual apparent strength shows a decreasing trend [28].

Until now, considerable research has been conducted on the cement-treated mixtures sub-base, and it has been used widely as an asphalt pavement base. However, under the condition of multi-factor interactions, the research on the anti-erosion behavior of a cement-treated mixtures sub-base is still inadequate. Using self-developed model testing, the cement-treated materials base's anti-erosion performance was studied in this paper by considering the variation in single factors first, then a prediction model of the erosion value of a cement-stabilized macadam base was studied with the Grey Theory under multi-factor conditions.

2. Materials and experimental methods

2.1. Cement

This study compared and analyzed the cementing material's influence on cement-treated mixtures' anti-erosion performance, and used P.O. 32.5 and P.O. 42.5 Portland cement produced by Conch Cement Company in China as the cementing agent. Table 1 presents the cement's main technical indicators that were

Table 1
Technical indicators of cementing agent.

Strength class	Fineness /%	Initial setting time /min	Final setting time /min	Soundness	Loss on ignition /%	Water content of standard consistence /%	28d compressive strength /MPa
32.5	3.8	171	228	Qualification	3.3	27.7	44.70
42.5	5.1	173	238	Qualification	5.0	28.0	51.15

Table 2
Passing rate of aggregate gradation.

Gradation type	The pass rate of the following sieves size/mm												
	31.5	26.5	19	16	13.2	9.5	4.75	2.36	1.18	0.6	0.3	0.17	0.075
XM	100	96.5	91.3	85	76	58.5	39	26	21	15	11	7	4
GM	100	90.5	78	67	58	46	27	20	15	9	4	2	0.5
GK	100	85	65	53	41	26	11	5	3	2	1	1	1

obtained through laboratory tests. The test method and sample preparation can be found in the Test Methods of Cement and Concrete for Highway Engineering (JTG F40-2004) [29].

2.2. Aggregates

In this paper, according to the structural types of a cement-treated mixtures sub-base recommended in the literature [30], and coarse mineral aggregate's distribution states in the mixtures, the cement-treated mixtures were divided into three structural types: "suspend-dense" structure (XM), "framework-dense" structure (GM), and "framework-pore" structure (GK), with a nominal maximum aggregate size of 31.5 mm (presented in Table 2), to analyze the gradation composition's influence on the mixtures' anti-erosion performance [31–34].

The aggregate and mineral filler used in the tests were purchased at a quarry, and the sandstone aggregate made according to different size standards was obtained after two steps of crushing, grinding, classification, and gravity separation. The aggregate and mineral powder's technical indicators are shown in Tables 3 and 4.

2.3. Water

Tap water was used in the experiments.

2.4. Manufacturing samples

The specific method used to prepare the specimens for the cement-treated mixtures scouring test was as follows: First, it weighed a certain amount of washed and dried aggregates in raw condition, cement and water accurately, and mixed them. Second, the mixtures were loaded into a mould ($\varnothing$150 mm × 350 mm) to make the specimens, and then compacted to 98% by a static pressure method [35]. To reduce the test data's error, three specimens were made under each working condition (see Fig. 1). Third, when the specimens removed from the mould and cured for 28 days in an incubator at 40 °C, 90% relative humidity, the volumetric performance test results for three structural types as shown in Table 5, and then were immersed in ambient temperature water for 1 day before testing. Finally, the specimens were frozen for 6 h at −5 °C in an indoor environment, and then placed in an outdoor environment (30°C) until the ice melted on the specimens' surface; this was repeated 5 times to simulate the environment's influence based on the project.

Table 3
Technical indicators of aggregate.

Detection Indicator	Test results	Properties	Test results
Water absorption/%	1.20	Specific gravity-apparent/(g·cm^{-3})	
Aggregate and asphalt adhesion/grade	5.40	10–20/cm	3.51
L.A. abrasion/%	20.43	5–10/cm	1.50
Flakiness/%	9.50	Stone chippings	1.43
Rock powder/(g·cm^{-3})	2.81		

Table 4
Technical indicators of mineral filler.

| Detection Indicator	Test results
Apparent relative density/(g·cm^{-3})	2.81
Water content/%	0.89
Appearance	No agglomeration
Hydrophilic coefficient	≤1

2.5. Testing instrument and conditions

Based on the analysis of the mechanism of scouring diseases in cement-treated mixtures, a scouring instrument composed of a scouring cylinder, rubber sleeve, controller, and air compressor was developed to conduct our in-depth study of Bao-han highway [23]. The instrument's working principle (as shown in Fig. 2) was as follows: First, it adjusted the degree of pressure in the scouring cylinder and placed the test specimen and a certain amount of water to the design value, such that the air pressure forces the plate inside the scouring cylinder to move downward, and then compresses the surface water on the specimen to simulate the scouring effect of water retained between the surface layer and cement-treated mixtures sub-base in the pavement when vehicle wheel load compresses the road surface. Second, it relieved the pressure gradually as it reached the design value, which caused the water around the specimen to move upward and exert suction on the specimen's surface to simulate the effect of "pump suction" on cement-treated materials that occurs when the vehicle's axle leaves the contact point with the road surface.

Fig. 1. Test specimens of different structural types of cement-treated mixtures.

Table 5
vol Index of cement-treated mixtures.

Volume index Structural types	Cement content/%	Max dry density/(g·cm^{-3})	Compressive strength/MPa	Optimal water content/%
XM	5	2.07	5.06	5.95
GM	5	2.19	5.18	5.45
GK	7	2.26	5.01	4.95
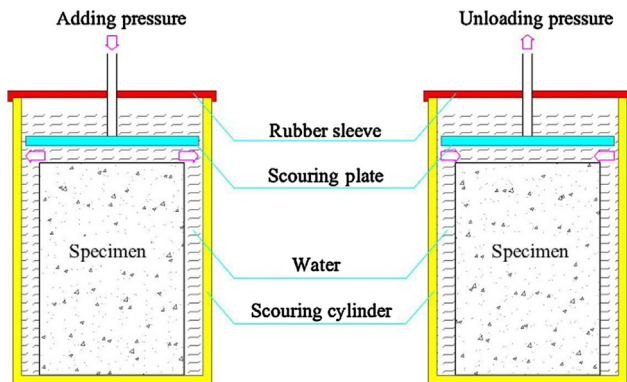
Fig. 2. Basic principles of scouring resistance test.

Fig. 3. The relation between scouring mass and cement content in cement-treated mixtures.
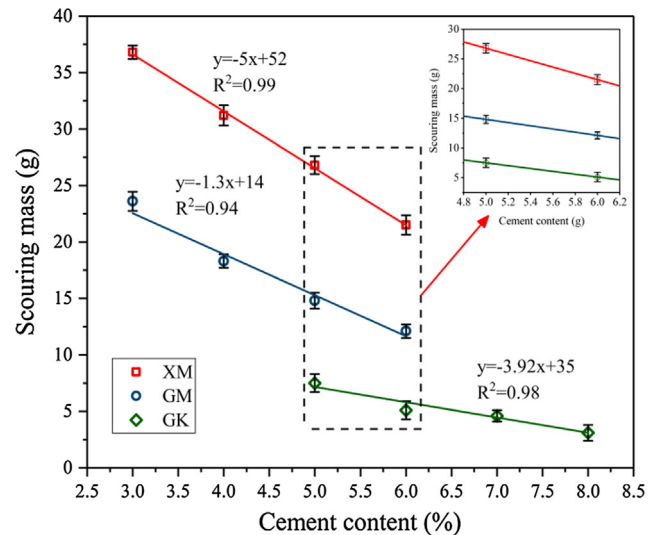
2.6. Experimental procedures

The process of the scouring test can be divided into four steps, as follows: First, after the freeze-thaw cycles, the specimens were weighed and fixed inside the scouring cylinder. This injects clean water of 30 into the cylinder, such that the water surface is 5 cm from the top of the specimen. Second, the following parameters were set on the controller: pressure (0.5 MPa), frequency (10 Hz), and scouring time (30 min). Third, after the end of the scouring test, the scoured mixtures were poured into a special container, and placed indoors for 12 h until the deposits separated from the mixtures and achieved full precipitation. The container with only scouring materials was placed in a dryer to dry to the optimum water content. Finally, the dry mixtures were weighed with an electronic balance to obtain the mass the cement-treated mixtures specimens lost.

3. Results and analysis

3.1. Cement content's influence on cement-treated mixtures' anti-erosion

The cement contents' effect on the cement-treated mixtures' anti-erosion performance was analyzed based on the previous results [28], in which matched specimens of gradations XM and GM were made with mixtures of 3%, 4%, 5% and 5% cement content. The specimens corresponding to gradation GK were made with mixtures of 5%, 6%, 7%, and 8% cement content. The results are shown in Fig. 3.

The results shown in Fig. 3 indicate that there is a strong linear correlation between the scouring mass and cement content of cement-treated mixtures with different structural types, with a correlation between the two up to 0.94, which shows that the cement binder affects the mixtures' scour resistance significantly. The results above show that with an increase in cement content, the cement-treated mixtures' degree of erosion decreased constantly. They also show that increasing the cement content in the mixtures improved the cement-treated mixtures' resistance to erosion for the following reason. For the XM and GM gradations, when the cement content in the mixtures is below 5% and 7%, respectively, the specific surface area of binder increased with increased cement usage. The larger the specific surface area of fillers per volume, the stronger the interfacial interaction and will be [36]. This caused the cohesion of fine aggregate and the adhesion force of fine aggregate on coarse aggregate to enhance, which reduced the like-

lihood of peeling under scouring force. However, above 5% and 7%, the range in the reduction in the amount of erosion was small as the cement content in the mixture increased. This indicates that when the cement content exceeded 5% and 7%, increasing it further contributed little to the improvement of the mixtures' erosion resistance, which is consistent with other research results [37].

3.2. Moisture content's influence on cement-treated mixtures' anti-erosion

This study also analyzed cement-treated mixtures moisture contents' effect on anti-erosion based on the previous result [28], in which the specimens were made with mixtures of 5.0%, 5.3%, 5.5% (GM), 5.7%, 5.5%, 5.8%, 6.0% (XM), and 6.2%, 4.5%, 4.8%, 5.0%, (GK), respectively, with 5.2% moisture content, and 5%, 5%, and 7% cement content based on the results of cement content's influence above. The results are shown in Fig. 4.

It can conclude from Fig. 4 that under the 3 gradation conditions, the scouring mass decreased firstly and increased thereafter with the increase in the mixture's water dosage, and reached its minimum value when the ratio of moisture content to mixture was optimum at a moisture content of 4.95%, 5.45%, and 5.95% for the GK, GM, and XM mixtures, respectively. The results above indicate that when the ratio is less than optimal, it is difficult to form a stable, compact structure between the coarse and fine aggregates because the aggregates' surface cannot be wrapped fully, and the aggregates cannot be squeezed and compacted because of insufficient cement mortar that cannot be hydrated completely because of the lack of moisture. In contrast, when the mixtures' moisture content exceeds the optimal value, their anti-erosion properties decrease, largely because of the structure's poor stability, in which the aggregates slide because a layer of excess water forms on the fine's surface. In addition, the formation of more voids in the specimens attributable to the evaporation of
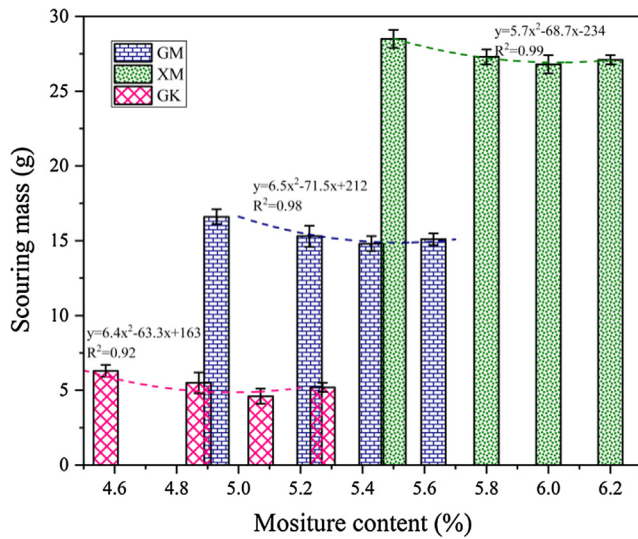
Fig. 4. The relation between scouring mass and moisture content in cement-treated mixtures.

Fig. 5. The relation between scouring mass and cement-treated mixtures' compaction.

the excess water reduces the mixtures' erosion resistance. Therefore, the materials' moisture content should be controlled strictly in applied engineering.

3.3. Compactness's influence on cement-treated mixtures' anti-erosion

Here, it selected 3 compactness conditions (Fig. 5) to analyze compactness's effect on the cement-treated mixtures' anti-erosion and the model test results, and the optimum water content (4.95%, 5.45%, and 5.95%) and cement dosage (5%, 5%, and 7%) determined in the tests above were used to make the specimens. The other test conditions were the same as those described in section 2. The test results are shown in Fig. 5 below.

Fig. 5 shows that, under the optimum water content and cement dosage conditions, as compactness increased, the XM mixture's scour mass decreased constantly, and decreased 6.8 g on average as the compactness increased 2%. This finding can be attributed to the fact that the content of fine aggregate in suspended dense structure mixtures is greater than that of coarse aggregate. With the increase in compactness, the voids between fine aggregates are squeezed gradually and filled by cement slurry, while the voids between coarse aggregates attributable to rubber cement formed from fine aggregates and cement slurry, compact the XM mixtures' structure overall and the scour mass decreases accordingly. It can conclude from Fig. 5 that, under the optimum water content and cement dosage conditions, the GM mixture's scouring mass decreased firstly and increased thereafter with increased compactness, and reached its minimum value when the compactness was 98%. The results above indicate that when compactness was less than 98%, the GM mixture's structural density increased gradually with increased compactness, which enhanced its anti-scouring ability and reduced the mixture's scouring mass. However, when the compactness increased from 98% to 100%, the load on the coarse aggregate's skeleton structure exceeded its bearing capacity, destroyed the structure, and reduced the GM mixture's stability, which caused the scouring mass to increase. As the GK mixture's compactness increased, its scouring mass increased as well, and increased 2.1 g on average as the compactness increased 2%. This finding can be attributed to the fact that the GK mixture contains less fine than coarse aggregate. The coarse aggregates were crushed by excessive compactness, and damaged the GK mixture's skeleton structure, which caused the
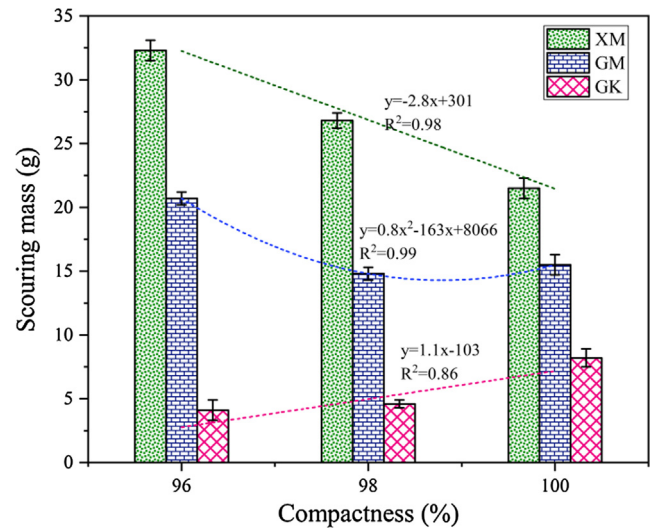
fine aggregates and crushed coarse aggregates to separate from the mixtures under the action of water flow scouring and increased the scouring mass greatly.

3.4. Structure-type's influence on cement-treated mixtures' anti-erosion

This study also analyzed structure's influence on cement-treated mixtures' anti-erosion performance. The three gradation mixtures (XM, GM, and GK) shown in Table 2 and the curing ages (3d, 7d, and 28d) were selected for mixtures with different types of structure. The cement dosage (5%, 5%, and 7%), water content (4.95%, 5.45%, and 5.95%) and compaction (100%, 98%, and 96%) determined in the tests above were selected to make the specimens to analyze structure type's influence on the cement-treated mixtures' anti-erosion. The other test conditions were the same as those described in section 2. The results are shown in Table 6 below.

The results in Table 6 show that the order of scouring mass of the 3 types of mixtures was $M_{XM} > M_{GM} > M_{GK}$ for the following reasons: the XM mixture has a remarkable characteristic, in that it contains more fine than coarse aggregate and the slurry mixture with fine aggregate and cement hydrate surrounds and separates the coarse aggregate, such that the coarse aggregate is like "isolated islands", and it is difficult to form a skeleton-embedded structure with less contact area. As a result, the fine aggregate bears the scouring force of water largely, which makes it easy for the fine aggregate to wash away, after which the coarse aggregate also washes. Thus, the XM mixture's scouring mass is greater than that of others. The GM mixture has a skeleton void structure formed by the interpenetration of coarse aggregates, in which mixtures of cement slurry and fine aggregates fill the voids and constrain the coarse aggregates and rubber cement mutually. The skeleton void structure bears the flow scouring force largely, which reduces the fine aggregates' erosion. The GK mixture's structure includes a greater amount of coarse than fine aggregate. Although it also has the skeleton void structure with coarse aggregates, the voids cannot be filled densely because of the lack of rubber cement, and the voids within the mixtures collude with each other, which weakens the flow scouring pressure and the scouring effect on fine aggregate. Thus, the GK mixture's scouring mass is lower than that of others. However, these mixtures have many voids that traffic

Table 6
Scouring test results of cement-treated mixtures with different structures.

Gradation type	Scouring mass/g			Total average error
	3d	7d	28d	
XM	30.1	22.7	18.8	0.62
GM	22.8	16.2	14.8	0.47
GK	12.1	7.3	4.1	0.50

Table 7
The scouring test results of cement-treated mixtures under different cement strength.

Gradation type	Cement content/%	Scouring mass/g		Total average error
		P.O. 32.5	P.O. 42.5	
XM	5.0	18.8	13.9	0.47
GM	5.0	14.8	10.8	0.55
GK	7.0	4.1	2.8	0.52

load and low scouring resistance damage easily. Therefore, it is suggested that GM mixtures should be used as the base in applied engineering.
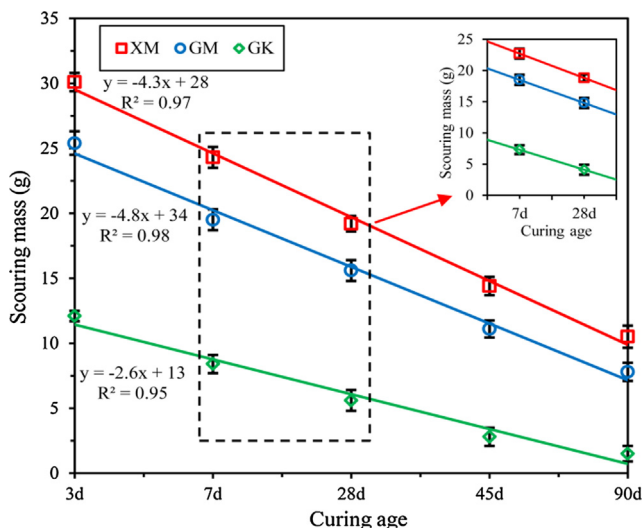
3.5. Curing age's influence on cement-treated mixtures' anti-erosion

In this test, 5 working conditions (3d, 7d, 28d, 45d, and 90d) were selected to analyze curing age's effect on cement-treated mixtures' anti-erosion and the model test results. The test results are shown in Fig. 6 below.

It can conclude from Fig. 6 that, under the conditions of different gradation, there is a strong linear correlation between cement-treated mixtures' scouring mass and curing age, in which the correlation coefficients exceeded 0.95. Under the 3 gradation conditions, the mixtures' scouring mass decreased with an increase in curing age, and the range decreased gradually. The average erosion reduction was 30.5%, 27.0%, 26.7%, and 16.5% with the 3 gradation mixtures (XM, GM, and GK) when the curing age increased from 3 d to 90 d, which demonstrates that the mixtures' base material's erosion resistance increased with increased curing age. This finding can be attributed to the fact that the low cement binder hydration produced only a small amount of cement slurry, which prevents the aggregates from bonding well, the mixtures' structure is loose as a whole, and the aggregates are washed away by the action of water pump easily with short curing age. As the curing age increases, the increased amount of cement hydrate increases the aggregates' cohesion and density, which enhances the mixtures' integrity, improves their anti-scouring ability, and decreases their scouring mass gradually.

3.6. Cement strength grade's influence on cement-treated mixtures' anti-erosion

In this study, Hailuo brand P.O.32.5 and P.O.42.5 cement (main indicators shown in Table 1) were selected to analyze cement

Fig. 6. The relation between scouring mass and curing ages in cement-treated mixtures.

strength grade's influence on the cement-treated mixtures' erosion resistance. Based on the results above and engineering practice, the optimum cement content of the 3 mixtures (XM, GM, and GK) was 5%, 5%, and 7%. The test results shown in Table 7 below were obtained by curing the specimens under standard conditions for 28 days.

Table 7 shows that with the same cement content, as the cement strength grade increased, the 3 gradation type cement-treated mixtures' scouring mass decreased with reduction ranges of 26.1%, 27.0%, and 31.7%, respectively, which indicates that the mixtures' scouring resistance improved because as the cement strength grade increases, the content of Portland in the cement binder increases. The content of cement slurry formed by cement hydrate and fine aggregate also increases, which increases the cohesion between fine aggregate and the adhesion of fine on coarse aggregate, the mixtures' strength overall, and thus, the mixtures' anti-scouring performance.

4. Grey relativity analysis of influencing factors and Grey modeling

4.1. Correlation between scouring mass and cement-treated mixtures' influencing factors

This study investigated and analyzed roadbed diseases that developed during the use of a highway in the Qinba Mountain area, Shaanxi Province, China, and the correlation between cement-treated mixtures' scouring mass and its primary influencing factors. Firstly, the fractal dimension (D) of mixtures with different structural types was calculated using the fractal theory to describe the 3 gradation mixtures' structural differences quantitatively. Secondly, the reference series was determined (Table 8) based on the results above of the tests of different influencing factors (cement dosage (P), water content, 28d cement mortar strength (f_{28}), compactness (C), fractal dimension (D), and cement strength grading (G)).

4.1.1. Averaging initial datas

Firstly, the initial series was determined with the scouring mass as the standard data array, and the cement dosage (P), water content (W), compaction (C), fractal dimension (D), cement strength grading (G), and cement mortar strength 28d(f_{28}) as the correlation data array, as shown in Table 3. Secondly, the initial sequence was averaged to generate the new standard and correlation data array as shown in Table 9.

4.1.2. Extremum values and resolution coefficient calculated

Based on the method of calculating the Grey correlation used in the literature [38], the two-level minimum and maximum values of the new series shown in Table 8 are, respectively: $minmin\Delta_i(k) = \{minmin|Y_0(k) - Y_i(k)||k = 1, 2, \cdots, 9; i = 1, 2, \cdots, 6\} = 0.0084$, $maxmax\Delta_i(k) = \{maxmax|Y_0(k) - Y_i(k)||k = 1, 2, L, 9; i = 1, 2, L, 6\} = 1.12$, such that the resolution coefficient of 0.5 was selected to calculate the two-level extremum.

Table 8
Scouring test results of the 3 gradation cement-treated mixtures.

Number	Gradation type	Scouring mass (M)/g	Influence factors					
			Cement dosage (P) /%	Water content (W) /%	Compaction (C) /%	Fractal dimension (D)	Cement strength grading (G)	28d cement mortar strength (f_{28})/Mpa
1	XM	36.1	4	5.1	100	2.4431	32.5	38.1
2		24.6	5	5.2	100	2.4431	32.5	38.4
3		21.5	6	5.5	100	2.4431	42.5	47.2
4	GM	23.6	4	5	98	2.3206	32.5	38.2
5		18.3	5	5.2	98	2.3206	32.5	38.5
6		14.4	6	5.5	98	2.3206	42.5	47.2
7	GK	11.5	3	4.9	96	2.0568	32.5	34.1
8		10.8	5	5.1	96	2.0568	32.5	38.5
9		8.2	7	5.5	96	2.0568	42.5	48.1

Table 9
Average processing results of initial data.

Indexes Number	M $x_0(k)$	P $x_1(k)$	W $x_2(k)$	C $x_3(k)$	D $x_4(k)$	G $x_5(k)$	f_{28} $x_6(k)$
1	1.92	0.80	0.98	1.02	1.07	0.91	0.93
2	1.31	1.00	1.00	1.02	1.07	0.91	0.94
3	1.14	1.20	1.05	1.02	1.07	1.19	1.15
4	1.26	0.80	0.96	1.00	1.02	0.91	0.93
5	0.97	1.00	1.00	1.00	1.02	0.91	0.94
6	0.77	1.20	1.05	1.00	1.02	1.19	1.15
7	0.61	0.60	0.94	0.98	0.90	0.91	0.83
8	0.58	1.00	0.98	0.98	0.90	0.91	0.94
9	0.44	1.40	1.05	0.98	0.90	1.19	1.18

4.1.3. Correlation between scouring mass and influencing factors calculated

The correlation coefficient between the influencing factors and the scouring mass under different test conditions was calculated with respect to the two-level extremum calculated above and the resolution coefficient determined. The results are shown in Fig. 7.

It can be seen from Fig. 7 that with the cement-treated mixtures' 3 gradation types, the order of the correlation coefficients between the influencing factors and the scouring mass was $\gamma_4 > \gamma_1 > \gamma_6 > \gamma_3 > \gamma_2 > \gamma_5$. Therefore, the mixtures' structure type had the most significant effect on their scour, followed by compactness, cement dosage, and 28d cement mortar strength. Water content had less effect, and cement strength grade the least for the

Fig. 7. Correlation coefficient between scouring mass and influencing factors.

following reason: Coarse aggregates in the mixtures are similar to the skeleton's effect in the human body. In mixtures in which the skeleton structure forms, the spaces between the aggregates are filled with fine aggregate and cement binder, which jointly resists the erosion of water flow in which its resistance depends on the mixtures' gradation type. Therefore, it can be seen that, compared with the other factors, the correlation was highest between the mixtures' fractal dimension (D) and their scour resistance. When the skeleton structure forms in the mixtures, its stability depends on the bond strength between the coarse and fine aggregates, which the mixtures' cement content (P) and 28d cement mortar strength (f_{28}) affect. It can be seen that the correlations between the mixtures' cement content, mortar strength, and scour resistance were similar. It can improve the cement-treated mixtures' anti-scouring ability by increasing the compaction (C). However, when the compaction is excessive, it will destroy their skeleton structure and reduce their anti-scouring ability. As Fig. 7 shows, the correlation between the mixtures' scouring mass and water content was close to that of compaction, and that between cement dosage and 28 cement mortar strength also was similar, while the correlation between cement strength grade and scouring mass was the lowest among the factors. Therefore, the main factors that affect the mixtures' erosion resistance are the gradation type, cement dosage, water content, and 28d cement mortar strength.

4.2. Prediction model of cement-treated mixtures' scouring mass

Based on these research findings and the research approach in the literature [24], the scouring mass prediction model of cement-treated mixtures was established with the parameters of aggregate fractal dimension (D), cement dosage (P), water content (W), 28d cement mortar strength (f_{28}), and compaction (C). The model was developed in the following steps:

4.2.1. Initial data processing and new data generation

Firstly, the data $x_i^{(0)}$ (shown in Table 10) were generated with a method of initializing the test data of the three gradation type mix-

Table 10
Results of initialization processing of initial data.

Parameters Number	M $x_0^{(0)}(k)$	P $x_1^{(0)}(k)$	W $X_2^{(0)}(k)$	C $X_3^{(0)}(k)$	D $X_4^{(0)}(k)$	f_{28} $X_5^{(0)}(k)$
$x_i^{(0)}$ (1)	1.00	1.00	1.00	1.00	1.00	1.00
$x_i^{(0)}$ (2)	0.681	1.25	1.02	1.00	1.00	1.01
$x_i^{(0)}$ (3)	0.596	1.50	1.08	1.00	1.00	1.24
$x_i^{(0)}$ (4)	0.654	1.00	0.98	0.98	0.95	1.00
$x_i^{(0)}$ (5)	0.507	1.25	1.02	0.98	0.95	1.01
$x_i^{(0)}$ (6)	0.399	1.50	1.08	0.98	0.95	1.24
$x_i^{(0)}$ (7)	0.319	0.75	0.96	0.96	0.84	0.90
$x_i^{(0)}$ (8)	0.299	1.25	1.00	0.96	0.84	1.01
$x_i^{(0)}$ (9)	0.227	1.75	1.08	0.96	0.84	1.26

Table 11
Results of accumulation processing of data x(0).

Parameters Number	M $x_0^{(1)}(k)$	P $x_1^{(1)}(k)$	W $X_2^{(1)}(k)$	C $X_3^{(1)}(k)$	D $X_4^{(1)}(k)$	f_{28} $X_5^{(1)}(k)$
$x_i^{(1)}(1)$	1.00	1.00	1.00	1.00	1.00	1.000
$x_i^{(1)}(2)$	1.68	2.25	2.02	2.000	2.000	2.008
$x_i^{(1)}(3)$	2.28	3.75	3.10	3.000	3.000	3.247
$x_i^{(1)}(4)$	2.93	4.75	4.08	3.980	3.950	4.249
$x_i^{(1)}(5)$	3.44	6.00	5.10	4.960	4.900	5.260
$x_i^{(1)}(6)$	3.84	7.50	6.18	5.940	5.850	6.499
$X_i^{(1)}(7)$	4.16	8.25	7.14	6.900	6.691	7.394
$x_i^{(1)}(8)$	4.45	9.50	8.14	7.860	7.533	8.404
$x_i^{(1)}(9)$	4.68	11.25	9.22	8.820	8.375	9.667

tures shown in Table 8. Secondly, the data $x_i^{(1)}$ (see Table 11) were established by the data's $x_i^{(0)}$accumulation generation operator (1-AGO).

4.2.2. Calculating sequence â

The sequence â was completed by the following calculation procedure. Firstly, it formed a sequence, $Z_1(^1(k)$, that can be calculated with Eq. (1), after which the matrix, B, was established with Eq. (2). The sequence Y_n stands for a data vector determined with Eq. (3) which was constituted with the data in Table 10, excluding the first row and column. Secondly, the sequence â was calculated with Eq. (4) which was based on the matrix, B, and sequence Y_n.

$$Z_1^{(1)}(k) = -\left[x_i^{(1)}(k-1) + x_i^{(1)}(k)\right]/2$$
$$= (-1.341, -1.979, -2.604, -3.184, -3.637, -3.996, -4.305, -4.568) \quad (1)$$

$$B = \begin{bmatrix} z_1^{(1)}(2) & x_1^{(1)}(2) & \cdots & x_5^1(2) \\ z_1^{(1)}(3) & x_1^{(1)}(3) & \cdots & x_5^1(3) \\ \vdots & \vdots & \vdots & \vdots \\ z_1^{(1)}(9) & x_1^{(1)}(9) & \cdots & x_5^1(9) \end{bmatrix}$$

$$= \begin{bmatrix} -1.341 & 2.250 & 2.020 & 2.000 & 2.000 & 2.008 \\ -1.979 & 3.750 & 3.098 & 3.000 & 3.000 & 3.247 \\ -2.604 & 4.750 & 4.078 & 3.980 & 3.950 & 4.249 \\ -3.184 & 6.000 & 5.098 & 4.960 & 4.900 & 5.260 \\ -3.637 & 7.500 & 6.176 & 5.940 & 5.850 & 6.499 \\ -3.996 & 8.250 & 7.137 & 6.900 & 6.691 & 7.394 \\ -4.305 & 9.500 & 8.137 & 7.860 & 7.533 & 8.404 \\ -4.568 & 11.250 & 9.216 & 8.820 & 8.375 & 9.667 \end{bmatrix} \quad (2)$$

$$Y_n = \left[x_1^{(0)}(2), x_1^{(0)}(3), x_1^{(0)}(4), x_1^{(0)}(5), x_1^{(0)}(6), x_1^{(0)}(7), x_1^{(0)}(8), x_1^{(0)}(9)\right]^T =$$
$$[0.681, 0.596, 0.654, 0.507, 0.399, 0.319, 0.299, 0.227]^T \quad (3)$$

$$\hat{a} = (B^T B)^{-1} B^T Y_n = [a, u]^T$$
$$= (5.913, 1.929, -27.229, 13.180, 14.416, 2.012)^T \quad (4)$$

in which: $Z_1^{(1)}(k)$ is a mean sequence formed from data $x_i^{(1)}(k-1)$ and $x_i^{(1)}(k)$ shown in Table 11. The data $x_i^{(0)}(k)$ are shown in Table 10. The "a" is the development coefficient, and the "u" is the driving coefficient in establishing the Grey model (GM) (1,6).

4.2.3. Calculating initial data time response $\hat{x}_1^{(1)}$

The differential equation of the GM (1,6) model shown in Eq. (6) can be established by substituting sequence â into Eq. (5), for which the approximate time response formula is formula (7).

$$x_1^{(0)}(k) + az_0^{(1)}(k) = \sum_{i=1}^{n} b_i x_i^{(1)}(k) \quad (5)$$

$$\frac{dx_1^{(1)}}{dt} + 5.913x_1^{(1)} = 1.929x_2^{(1)} - 27.229x_3^{(1)} + 13.18x_4^{(1)}$$
$$+ 14.416x_5^{(1)} + 2.0126x_6^{(1)} \quad (6)$$

$$\hat{x}_1^{(1)}(k+1) = (x_1^{(1)}(0) - \frac{1}{a}\sum_{i=1}^{n} b_i x_i^{(1)}(k+1))e^{-ak} + \frac{1}{a}\sum_{i=1}^{n} b_i x_i^{(1)}(k+1)$$
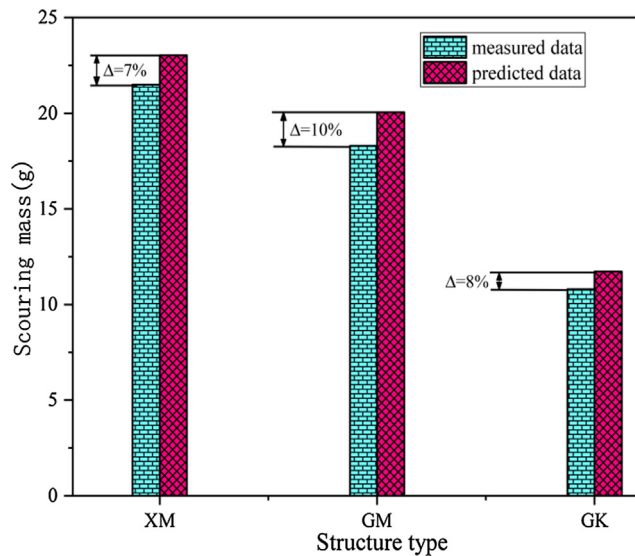$$= \left[1 - 0.169\sum_{i=1}^{5} b_i x_i^{(1)}(k+1)\right]e^{-0.169k}$$
$$+ 0.169\sum_{i=1}^{5} b_i x_i^1(k+1) \ (k = 0, 1, 2, \ldots 8) \quad (7)$$

The response values of the data in the principal sequence of actions are $\hat{x}_1^{(1)} = (1.00, 1.45, 2.06, 2.72, 3.27, 3.72, 4.03, 4.37, 4.60)$. The response values of the initial data are $\hat{x}_1^{(0)} = (36.10, 20.2, 22.13, 23.57, 20.09, 16.06, 11.45, 12.24, 8.18)$, which can be obtained by the inverse calculation of the 1-AGO and initialization of sequence $\hat{x}_1^{(1)}$.

Table 12
Calculating parameters of mixtures with different structural types.

Structure type	P/%	W/%	C/%	D	f_{28}/ Mpa
XM	6.0	5.5	100	2.4431	47.2
GM	5.0	5.2	98	2.3206	38.5
GK	5.0	5.1	96	2.0568	38.5

Fig. 8. Relative errors between measured and predicted data.

4.2.6. Model validation

In this section, 3 structural types of cement stabilized macadam (XM, GM, GK) are selected to test the prediction model of cement-treated mixtures' scouring mass. The calculated parameters of mixtures with different structural types are shown in Table 12. The relative errors between measured and predictive data are shown in Fig. 8.

It can conclude from Fig. 8 that, the relative error between measured and predicted data of the cement-treated mixtures with different structural types was less than 10%, which met the demands of codes and standards (≤20%) [35]. It shows that the discreteness of the predicted value was relatively small and in good agreement with the measured value. So the model can be used for prediction on the cement-treated mixtures' scouring mass.

5. Conclusions and suggestions

In this paper, the anti-erosion performance and mechanisms of sub-bases composed of different cement-treated mixtures were investigated systematically and thoroughly through self-developed laboratory tests under different influencing factors. The main conclusions are as follows:

(1) A strong correlation was found between cement-treated mixtures' scour resistance and cement dosage, strength grade, and curing age, and the mixtures' anti-erosion ability increased with increased cement binder content, strength grade, and curing age.
(2) Cement-treated mixtures' erosion resistance was related to water content and their degree of compaction. When water content and compactness were significantly more or less than optimal, it failed to improve cement-treated mixtures sub-base's erosion resistance. Therefore, cement-treated mixtures' water content and compactness should be controlled strictly in applied engineering.
(3) Under the same test conditions, the 3 mixtures' order of scour resistance was "suspend-dense" (XM), "framework-dense" (GM), and "framework-pore" structure (GK). Thus, it is suggested that the "framework-dense" structure should be prioritized in applied engineering.
(4) A prediction model of cement-treated mixtures' scouring mass was established with the parameters of aggregate fractal dimension, cement dosage, water content, 28d cement mortar strength, and compactness, which reflected the mixtures' scour resistance, and provides design and construction guidance for similar projects.

4.2.4. Establishing the prediction model of the cement-treated mixtures' scouring mass

According to the results above, the calculation model for the mixtures' scouring mass was established with the parameters of aggregate fractal dimension (D), cement dosage (P), water content (W), 28d cement mortar strength(f_{28}), and compaction (C), which is shown as equation (8),

$$\hat{x}_0^{(1)}(k+1) = \left[1 - 0.169 \sum_{i=1}^{5} b_i x_i^{(1)}(k+1)\right] e^{-0.169k} + 0.169 \sum_{i=1}^{5} b_i x_i^{(1)}(k+1)$$
$$k \geq 9$$
$$\hat{x}_0^{(0)}(k+1) = \left[\hat{x}_0^{(1)}(k+1) - \hat{x}_0^{(1)}(k)\right] \times 36.1$$

(8)

in which: $\hat{a} = (a, b_1, b_2 ..., b_6)^T = (5.913, 1.929, -27.229, 13.180, 14.416, 2.012)^T$

4.2.5. GM (1,6) precision check

Here, the residual verification was checked and thereafter, difference verification of the model established was assessed. (1) Residual verification. The established model's relative error sequence is $\Delta = (\Delta_1, \Delta_2, ... \Delta_{10}) = (0, 17.9\%, 3\%, 0, 10\%, 12\%, 0, 13\%, 0)$, and the average relative error between the cement-treated mixtures' predicted scouring mass and the actual value was 6.2%, which was less than 20%, and thus met the demands of codes and standards [35]. (2) Subsequent check of difference verification. The mean square deviations of the initial sequence (S_2) and residual series (S_1) were calculated as 1.75 and 9.88, respectively. The calculated mean square error ratio was 0.18, which can be obtained with formula (9). (3) The small error probability. Using formula (10), the probability of small error calculated was 1. Therefore, based on [38], the precision grade of the model of cement-treated mixtures' scouring mass is one.

References

[1] Grili, E. Bocci, A. Graziani, Influence of reclaimed asphalt content on the mechanical behavior of cement-treated mixtures, Road. Mater. Pavement Des. 14 (3) (2013) 666–678.

[2] A. Arulrajah, M.M. Disfani, S. Horpibulsuk, C. Suksiripattanapong, N. Prongmanee, Physical properties and shear strength responses of recycled construction and demolition materials in unbound pavement base/sub-base applications, Constr. Build. Mater. 58 (15) (2014) 245–257.

[3] AASHTO, Guide for Design of Pavement Structures, American Association of State Highway and Transportation Officials, USA: Washington, DC, 1993.

[4] M. De Beer, Aspects of the design and behavior of road structures incorporating lightly cementitious layers Doctoral Dissertation, University of Pretoria Pretoria, 1990.

[5] D.X. Xuan, L.J.M. Houben, A.A.A. Molenaar, Z.H. Shui, Mechanical properties of cement-treated aggregate material-a review, Mater. Des. 33 (1) (2013) 496–502.

[6] C. Jaysinghe, R.S. Mallawaarachchi, Flexural strength of compressed stabilized earth masonry materials, Mater. Des. 30 (9) (2009) 3859–3868.

[7] D.X. Xuan, L.J.M. Houben, A.A.A. Molenaar, Z.H. Shui, Mixture optimization of cement-treated demolition waste with recycled masonry and concrete, Inter. J. Mater. Struct. 45 (1–2) (2012) 143–151.

[8] L.Q. Hu, J.X. Hao, L.B. Wang, Laboratory evaluation of cement-treated aggregate containing crushed clay brick, J. Traf. Tran. Eng. 1 (5) (2014) 371–382.

[9] P. Paige-Green, C. Ware, Some material and construction aspects regarding in situ recycling of road pavements in South Africa, Road. Mater. Pavement Des. 7 (3) (2006) 273–287.

[10] K. Siripum, P. Jitsangiam, H. Nikraz, Characterization analysis and design of hydrated cement-treated crushed rock base as a road base material in Western Australia, Inter. J. Pavement Res. Tech. 2 (6) (2009) 257–263.

[11] F.G. Bell, Engineering Treatment of Soils, E & FN Spon, London, England, 1993, pp. 99–135.

[12] National Institute for Transport and Road Research, Cementitious Stabilizers Inroad Construction, Committee of State Road Authorities, Pretoria, South Africa, 1986.

[13] J.L. Zheng, New concept of durable asphalt pavement design based on increasing structural layer life, China. J. High. Transp. 27 (1) (2014) 1–7.

[14] X. Yang, Z.P. You, J. Hiller, Sensitivity of flexible pavement design to Michigan's climatic inputs using pavement ME design, Int. J. Pavement Eng. 18 (7) (2015) 622–632.

[15] J.P. Zhang, S.C. Cui, J. Cai, J.Z. Pei, Y.S. Jia, Life-cycle reliability evaluation of semi-rigid materials based on modulus degradation model, KSCE. J. Civ. Eng. 22 (6) (2018) 2043–2054.

[16] A.M. Sha, S. Tu, Cracks Characteristics and Damage Mechanism of Asphalt Pavement with Semi-Rigid Base, 7th RILEM International Conference on Cracking in Pavements, Delft, Netherlands, 2012.

[17] J. Kennedy, Cement-Bound Materials for Sub-bases and Road Bases, Cement and Concrete Association Publication, Slough, England, 1983.

[18] S. Kolias, K.A. Davis, L.S. Warr, E.J. Hoppe, Physical and chemical behavior of four cement-treated aggregates, J. Mater. Civil. Eng. 19 (2007) 891–897.

[19] G.W. White, C.T. Gnanendran, The influence of compaction method and density on the strength hand modulus of cementitiously stabilised pavement materials, Inter. J. Pavement Eng. 6 (2) (2005) 97–110.

[20] P. Kumar Mehta, J.M. Monteriro Paulo, Concrete, microstructure, properties, and materails, McGrwa-Hill, Newyork, America, 2006.

[21] S.G. Hu, Y.H. Zhang, F.Z. Wang, Effect of temperature and pressure on the degradation of cement asphalt mortar exposed to water, Constr. Build. Mater. 34 (2012) 570–574.

[22] S.L. Li, G.M. Sheng, H.S. Shi, Acoustic emission characteristics of semi-rigid bases with three moisture conditions during bending tests, Road. Mater. Pavement Des. 2 (2017) 1–12.

[23] Y.P. Sheng, S.F. Chen, D. Wang, L.B. Wang, Pore water pressure characteristics of semi-rigid base for cement concrete pavement, KSCE. J. Traf. Trans. Eng. 12 (1) (2012) 6–12.

[24] A.M. Sha, Material characteristics of semi-rigid base, China. J. Highway Transp. 21 (1) (2008) 1–5.

[25] V. Alexandria, Soil and Pavement Base Stabilization with Self-Cementing Coal Fly Ash, Coal Ash Association International, American, 1999.

[26] M.J. Zhang, H. Guan, H.J. Liang, The study on the anti-brushing performance of semi-rigid base course, J. Shenyang Jianzhu Univ. 22 (3) (2006) 371–374.

[27] P. Majarrea, Fernando, Semi-rigid pavement performance and construction techniques for semiarid areas, Road Mater. Pavement Des. 14 (3) (2014) 615–637.

[28] R. Guo, H. Jiang, C. Liu, W.Y. Chen, Experimental study on anti-erosion performance of semi-rigid base for asphalt pavement, J. Shaanxi Univ. Tech. 34 (3) (2018) 17–21.

[29] Ministry of Transport of the People's Republic of China, Test Methods of Cement and Concrete for Highway Engineering JTG, Communication Press, Beijing, China, 2006, pp. E30-2005.

[30] M.J. Si, X.Y. Li, H.T. Li, Analysis on key points of construction quality control and mix proportion design of cement stability crushed stone in expressway, Highway Eng. 42 (6) (2017) 119–300.

[31] Y. Sun, L.H. Li, Strength assessment and mechanism analysis of cement stabilized reclaimed lime-fly ash macadam, Constr. Build. Mater. 166 (2018) 118–129.

[32] X.D. Zhang, K. Ren, Strength and damage characteristic of cement stabilized cinder macadam base, J. Traff Transp. Eng. 18 (6) (2018) 1–9.

[33] Y.P. Sheng, L.L. Li, B.W. Guan, H.L. Zhou, R. H, H.X. Chen, Study on the performance of gravel road stabilized by early strength agent and brucite fibers in alpine regions, J. Glaciol Geocr. 40 (2) (2018) 355–361.

[34] Ministry of Transport of the People's Republic of China, Specifications for design of highway asphalt pavement, Communication Press, Beijing, China, 2017, pp. D50-2017.

[35] Ministry of Transport of the People's Republic of China, Test Methods of Materials Stabilized with Inorganic Binders for Highway Engineering JTG, Communication Press, Beijing, China, 2009, pp. E51-2009.

[36] M. Guo, Y.Q. Tan, Interaction between asphalt and mineral fillers and its correlation to mastics' viscoelasticity, Inter. J. Pavement Eng. (2019) 1–10, https://doi.org/10.1080/10298436.2019.1575379.

[37] T.L. Zhu, Z.M. Tan, Y.M. Zhou, Experimental research on erosion-resistance performance of semi-rigid base materials, J. Build. Mater. 16 (4) (2013) 608–613.

[38] J.L. Deng, Grey Theory Basis, Huazhong University of Science and Technology Press, Wuhan, China, 2002, pp. 108–177.